

PHYSICAL REVIEW C **87**, 065803 (2013)**Shell-model studies of the astrophysical  $rp$  reaction  $^{29}\text{P}(p,\gamma)^{30}\text{S}$** W. A. Richter<sup>1,2,\*</sup> and B. Alex Brown<sup>3</sup><sup>1</sup>*Themba LABS, P. O. Box 722, Somerset West 7129, South Africa*<sup>2</sup>*Department of Physics, University of the Western Cape, Private Bag X17, Bellville 7535, South Africa*<sup>3</sup>*Department of Physics and Astronomy, and National Superconducting Cyclotron Laboratory, Michigan State University, East Lansing, Michigan 48824-1321, USA*

(Received 19 February 2013; revised manuscript received 2 May 2013; published 25 June 2013)

We present results for levels in  $^{30}\text{S}$  (the mirror nucleus of  $^{30}\text{Si}$ ) that are used for the  $^{29}\text{P}(p,\gamma)$   $rp$  reaction rate calculations. The resonance energies used in the reaction rate calculations are based on recent measurements which extend the excitation energy spectrum. The levels are checked against results from the isobaric mass multiplet equation and the binding energies of the  $T = 1$  analog states. Where the analog states are not known the levels are calculated with two-body interactions that use the  $sd$ -shell interactions USDA and USDB as the charge-independent parts, with a Coulomb, charge-dependent, and charge-asymmetric Hamiltonian added. The  $\gamma$ -decay lifetimes and  $^{29}\text{P}$  to  $^{30}\text{S}$  spectroscopic factors are also calculated with the same interactions, and together with experimental information on the levels of excited states are used to determine the  $^{29}\text{P}(p,\gamma)^{30}\text{S}$  reaction rates.

DOI: [10.1103/PhysRevC.87.065803](https://doi.org/10.1103/PhysRevC.87.065803)

PACS number(s): 26.30.-k, 21.60.Cs, 21.10.Sf, 21.10.Tg

**I. INTRODUCTION**

In explosive stellar environments, such as classical novae and x-ray bursters, thermonuclear radiative capture reactions on unstable nuclei determine the path of nucleosynthesis towards the proton drip line. These processes are often dominated by resonant capture to excited states above the particle-emission threshold and therefore depend critically on the nuclear properties of the levels involved.

In the case of the  $rp$  reaction  $^{29}\text{P}(p,\gamma)^{30}\text{S}$  most of the important energies and  $J^\pi$  assignments in the resonance region of importance have been provided by recent measurements [1,2].

The isobaric mass multiplet equation (IMME) affords a reliable method of obtaining levels in the ( $T_z = -1$ ) nuclei for the ( $p,\gamma$ ) reactions in terms of the isobaric analog partners and a IMME coefficient  $c$  that can be calculated [3]. The ( $p,\gamma$ ) rate depends on the proton-decay and  $\gamma$ -decay widths that are often not measured experimentally. Values obtained from the nuclear shell model can be used if the experimental levels can be matched with their theoretical counterparts. In this paper we use the  $sd$ -shell model space with the charge-independent interactions USDA and USDB [4] supplemented by Coulomb and charge-dependent interactions obtained in Ref. [5]. In this paper we consider the  $^{29}\text{P}(p,\gamma)^{30}\text{S}$  reaction. In Sec. II the properties of the  $T = 1$  triplets are discussed and used to establish the connection between experimental and theoretical levels. Also the experimental spectroscopic factors and  $\gamma$ -decay properties of the mirror levels in  $^{30}\text{Si}$  are compared with the theory. In Sec. III the result for the  $^{29}\text{P}(p,\gamma)^{30}\text{S}$  rate is given with an evaluation of its uncertainties. The conclusions are presented in Sec. IV.

**II. PROPERTIES OF THE ISOBARIC TRIPLETS FOR  $A = 30$** 

Because of the exponential dependence of the reaction rate on the resonance energy of the final nucleus of the ( $p,\gamma$ ) reaction [16], it is imperative to use as accurate energies as possible. There are three different sources for the energies that are generally input into reaction rate calculations: (1) well-established experimental energies; (2) predicted levels based on the IMME to calculate the expected energy of levels in  $^{30}\text{S}$  by using the measured binding energies of the  $T = 1$  partners and a theoretical value of the  $c$  coefficient of the IMME [5]; (3) level energies calculated with reliable  $sd$ -shell two-body interactions such as USDA and USDB.

Energies and  $J^\pi$  assignments for states above the proton-emission threshold have been obtained by recent measurements from Setoodehnia *et al.* [7], Lotay *et al.* [2], and Almaraz-Calderon [1]. This covers the region of the most important resonances.

The IMME equation is

$$B(T_z) = a + bT_z + cT_z^2, \quad (1)$$

where  $B$  is the binding energy of a state. Given the energies for isobaric triplets  $T_z = 1, 0,$  and  $-1$  ( $^{30}\text{Si}$ ,  $^{30}\text{P}$ , and  $^{30}\text{S}$  in this case) one can solve for  $c$ :

$$c = [B(T_z = -1) + B(T_z = 1)]/2 - B(T_z = 0). \quad (2)$$

In this mass region the properties of the  $T_z = 1$  nuclei ( $^{30}\text{Si}$  in this case) are the most well-established members of the  $T = 1$  multiplets. If the energies for  $T_z = 0$  ( $^{30}\text{P}$ ) are known from experiment then one can use

$$B(T_z = -1) = 2B_{\text{exp}}(T_z = 0) - B_{\text{exp}}(T_z = 1) + 2c_{\text{th}}. \quad (3)$$

to obtain the energy for  $T_z = -1$  ( $^{30}\text{S}$ ), where  $c_{\text{th}}$  is a relatively small number that can be calculated. In previous papers we have successfully used this method to predict energies and confirm spin assignments for the levels in the  $T_z = -1$  nuclei  $^{26}\text{Si}$  [3] and  $^{36}\text{K}$  [8]. Our initial plan was to use Eq. (3) to predict

\* richter@sun.ac.za

TABLE I. Energy levels of the  $T = 1$  isobaric analog states in  $A = 30$ , and experimental and theoretical  $c$  coefficients of the IMME in keV. Excitation energies are given in keV. Error margins are given only when they exceed a few keV. The multiplicity of the states  $k$  is determined by USDB-cdpn, and the state number  $n$  is in order of increasing energy for  $^{30}\text{Si}$ , where possible. The other references for the experimental data are discussed in the text. The negative-parity levels indicated by an asterisk have energies in  $^{30}\text{S}$  estimated from IMME systematics as described in the text.

$n$	$J^\pi$	$k$	$^{30}\text{P}$	$^{30}\text{Si}$	$^{30}\text{P} - 677 \text{ keV}$	$^{30}\text{S}$	$^{30}\text{S}$	$c$	$c$
			exp	exp	exp	exp	USDB-cdpn	exp	USDB-cdpn
1	0 <sup>+</sup>	1	677	0	0	0	0	276	280
2	2 <sup>+</sup>	1	2937	2235	2260	2210	2244	239	240
3	2 <sup>+</sup>	2	4182	3498	3505	3404	3485	222	240
4	1 <sup>+</sup>	1	4502	3769	3825	3677	3976	174	175
5	0 <sup>+</sup>	2	4468	3788	3791	3668	3871	212	210
6	2 <sup>+</sup>	3	5576	4810	4899	4809	4805	186	185
7	3 <sup>+</sup>	1	5509 (2,3)	4830	4832	4688	4825	201	220
8	3 <sup>+</sup>	2	6006 (3 <sup>+</sup> )	5231	5329 (3 <sup>+</sup> )	5219	5111	172	190
9	4 <sup>+</sup>	1	5934 (3 <sup>+</sup> )	5279	5257 (3 <sup>+</sup> )	5132	5278	223	235
10	0 <sup>+</sup>	3	6050(10) <sup>a</sup>	5372	[5373(10)] <sup>a</sup>	5218	5487	198(10)	235
11	3 <sup>-</sup>	1	6093	5487	5414	5312		260	
12	2 <sup>+</sup>	4	6268 (2 <sup>-</sup> )	5614	5593	5382	5867	181	195
13	4 <sup>+</sup>	2	6597	5951	5921	5836	5860	248	245
14	4 <sup>-</sup>	1	7049	6503	6372	(6225) *			
15	2 <sup>+</sup>	5		6537			6497		
16	2 <sup>-</sup>	1	7223 (2 <sup>-</sup> )	6641	6546 (2 <sup>-</sup> )	(6435) *			
17	0 <sup>+</sup>	4	7207 (0 <sup>+</sup> )	6642	6530	6326	6725	236	250
18	1 <sup>-</sup>	1	7178 (1 <sup>-</sup> )	6744	6501 (1 <sup>-</sup> )	(6242) *			
19	3 <sup>+</sup>	3		6865			6940		
20	2 <sup>+</sup>	6		6915 (2 <sup>+</sup> )			7024		
21	5 <sup>+</sup>	1		6999			6996		

<sup>a</sup>Reference [6].

energies and confirm spin assignments in  $^{30}\text{S}$ . However, based on the recent data for  $^{30}\text{S}$  we found several inconsistencies when using the proposed experimental  $T = 1$  assignments for levels above five MeV in  $^{30}\text{P}$ . Thus, for  $A = 30$  we start with an investigation of the ( $J^\pi$ ,  $T$ ) assignments for levels in  $^{30}\text{P}$ .

For the calculation of the  $b$  and  $c$  coefficients of the IMME we use the USDA and USDB Hamiltonians [4] for the charge-independent part and add the Coulomb, charge-dependent, and charge-asymmetric nuclear Hamiltonian obtained by Ormand and Brown for the  $sd$  shell [5]. These composite interactions are called USDA-cdpn and USDB-cdpn. The cd refers to charge-dependent, and pn indicates that the calculations are done in the proton-neutron formalism.

For the nuclei considered in Ref. [5],  $A = 18$ –22 and  $A = 34$ –39, the 42  $b$  coefficients were reproduced with an rms deviation of 27 keV and the 26  $c$  coefficients were reproduced with an rms deviation of 9 keV. There is considerable state-dependence in the  $c$  coefficients (ranging in values from 130 keV to 350 keV) that is nicely reproduced by the calculations (see Fig. 9 in Ref. [5]). This IMME method was used in Ref. [9] for the  $T = 1$  states of the odd-odd nuclei with mass 28, 32, and 36.

In Table I a summary is given of the  $T = 1$  triplets for  $A = 30$ . Experimental energies for  $^{30}\text{Si}$  and  $^{30}\text{P}$  are taken from the Nuclear Data Sheets (NDS) [10] unless otherwise indicated. The levels are numbered by  $n$  according to their well-established ordering in  $^{30}\text{Si}$ . The levels for a given  $J^\pi$  value are numbered by  $k$ . The  $^{30}\text{P}$  energies and  $J^\pi$  for the

states below 5 MeV, as well as the  $3^+$  ( $n = 8$ ,  $k = 2$ ) level at 5219 keV are taken from Lotay *et al.* [2]. The energies and  $J^\pi$  values for other states above 5 MeV are taken from Almaraz-Calderon *et al.* [1]. Above 6 MeV there are many states in  $^{30}\text{S}$  whose  $J^\pi$  values are uncertain. The states between 6 and 7 MeV given in Table I are those expected from the well-known levels in  $^{30}\text{Si}$ .

The  $T = 1$  levels in  $^{30}\text{P}$  appear to be well established up to  $n = 6$ . The experimental and theoretical  $c$  coefficients for the corresponding states in  $^{30}\text{S}$  are given in Table I and plotted in Fig. 1. Results for both USDA-cdpn and USDB-cdpn shown in Fig. 1 give some indication of the theoretical uncertainties. Given these uncertainties the experimental and theoretical  $c$  coefficients are in good agreement up to  $n = 6$ .

The level at 5.509 MeV in  $^{30}\text{P}$  has an assignment of  $J = (2, 3)$ ,  $T = 1$  in the NDS [10] and  $3^+$ ,  $T = 0$  in Ref. [11]. But the  $\gamma$  decay of this state is consistent with the USDB calculation for the  $3^+$ ,  $T = 1$  ( $n = 7$ ) state. Making this assignment gives reasonable agreement with theory for the  $c$  coefficient of the IMME (Fig. 1). Reference [11] is a “Complete Spectroscopy of  $^{30}\text{P}$ ”. But many of the adopted  $J^\pi$ ,  $T$  assignments given in Table V of that paper are based upon an assumed matching with the USD shell model [12] as well as a comparison with levels in  $^{30}\text{Si}$ . In this case and a few others we suggest changes to these model-dependent assignments. We note that the  $3^+$ ,  $T = 1$  theoretical level at 5.654 MeV in Table V of Ref. [11] is the only  $T = 1$  state in this energy region that did not have a previous association with experiment.

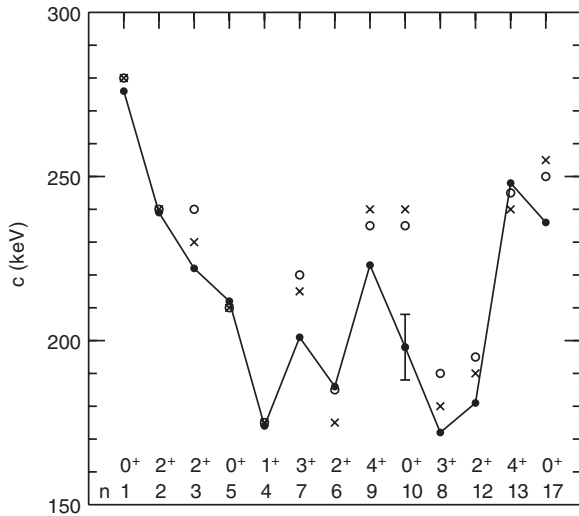


FIG. 1.  $c$  coefficients from the isobaric mass multiplet equation (IMME:  $E = a + bT_z + cT_z^2$ ) for states in  $^{30}\text{S}$  (in order of increasing experimental energy, as in Table I). The coefficients are experimental (closed circles) and theoretical, calculated from USDB-cdpn (open circles) and USDA-cdpn (crosses).

The level at 6.006 MeV in  $^{30}\text{P}$  has an assignment of ( $3^+$ ,  $T = 0, 1$ ) in the NDS [10] and  $3^+$ ,  $T = 0$  in Ref. [11]. But its gamma decay is consistent with the one calculated for  $3^+$ ,  $T = 1$   $n = 8$ . Making this assignment gives reasonable agreement with theory for the  $c$  coefficient. In Ref. [11] there is a level at 5.890(12) MeV that is associated with a  $3^+$ ,  $T = 1$  state. The nearest level in the NDS [10] is at 5.896(5) that is assigned ( $2^-$ ).

The theoretical  $4^+$  ( $n = 9$ ,  $k = 1$ ) level is the only state in this energy range of  $^{30}\text{P}$  that theoretically has a strong gamma-decay branch to the  $5^+$   $T = 0$  level (28% with USDB). The experimental level at 5.934 MeV in  $^{30}\text{P}$  with a ( $3^+$ ) spin assignment and no isospin assignment is observed to have a strong gamma branch of 42(1)% to the  $5^+$  [11]. The observed  $\gamma$ -decay pattern of this 5.934 MeV state is consistent with the one calculated for the  $4^+$  state. In addition, if we take the 5.934 MeV state in  $^{30}\text{P}$  to be the  $4^+$  member of the  $T = 1$  multiplet, the experimental  $c$  coefficient is consistent with theory (Fig. 1). Therefore, we suggest a  $4^+$ ,  $T = 1$  assignment to the 5.934 MeV state in  $^{30}\text{P}$ .

A level at 6.051 MeV in  $^{30}\text{P}$  is assigned ( $3,4,5$ )<sup>+</sup>,  $T = 1$  in the NDS [10] and  $4^+$ ,  $T = 1$  in Ref. [11]. However, with our association of the  $3^+$  and  $4^+$   $T = 1$  states with other levels, this level should not have  $T = 1$ . We note that many of the  $T = 1$  “assignments” are based upon previous suggestions for the plausible IMME associations based on the energies.

The next  $T = 1$  level is the  $0^+$  ( $n = 10$ ) state. No level in the NDS [10] has this assignment. But in a  $^{30}\text{Si}(t, ^3\text{He})^{30}\text{P}$  experiment [6] a level at 6.050(10) MeV is assigned ( $0,1$ )<sup>+</sup>, ( $T = 1$ ). The experimental  $\gamma$  decay of this level is not known. The resulting experimental  $c$  coefficient is not in very good agreement with theory (Fig. 1). Thus the correct experimental position of this  $0^+$ ,  $T = 1$  state in  $^{30}\text{P}$  is less certain than the cases discussed previously.

The next state with  $n = 11$  is the  $3^-$ . This  $T = 1$  multiplet of states appears to be fairly well established and we obtain an experimental  $c$  coefficient with a reasonable value of 260 keV. This is the first  $T = 1$  level that lies outside the sd shell model. To obtain energies for the experimentally uncertain higher negative-parity states in  $^{30}\text{S}$  ( $4^-$ ,  $2^-$ , and  $1^-$ ) we use Eq. (3) with their suggested energies in  $^{30}\text{Si}$  and  $^{30}\text{P}$  together with  $c = 260$  keV. For the  $rp$  reaction rate the experimental gamma widths and spectroscopic factors in the mirror nucleus  $^{30}\text{Si}$  are used.

The next state with  $n = 12$  is the  $2^+$ ,  $T = 1$  that is known in  $^{30}\text{Si}$  and has a suggested energy of 5.382 MeV in  $^{30}\text{S}$ . Best agreement with the theoretical  $c$  coefficient is obtained if we use the 6.268 MeV level in  $^{30}\text{P}$  that is assigned ( $2^-$ ),  $T = 1$  in the NDS [10] and  $2^-$ ,  $T = 1$  in Ref. [11]. This is a tentative  $T = 1$  triplet assignment.

The next state with  $n = 13$  is the  $4^+$ ,  $T = 1$  that is experimentally known in  $^{30}\text{Si}$  and  $^{30}\text{S}$ . There is a state at 6.598 MeV in  $^{30}\text{P}$  that is assigned ( $3,4^+,5^+$ ) in the NDS [10] and  $4^+$ ,  $T = 1$  in Ref. [11]. The experimental  $c$  coefficient of 248 keV obtained with this latter triplet association is in good agreement with theory (245 keV).

Starting with the  $2^+$   $n = 15$  state the associated energies of states in  $^{30}\text{P}$  and  $^{30}\text{S}$  are not known. There is a state at 6.656(5) MeV assigned  $2^+$ ,  $T = 1$  in Ref. [11], but it is about 500 keV too low to be associated with the  $2^+$   $n = 15$  state in  $^{30}\text{Si}$  and is too high to be associated with the  $2^+$   $n = 12$  state discussed above. Thus, it is probably an incorrect assignment.

The  $0^+$   $n = 17$  is the last one for which all members of the triplet can be established. Using the 7.207 MeV state assigned  $0^+$ ,  $T = 1$  in Ref. [11] we obtain  $c_{exp} = 236$  keV compared to the theoretical value of 250 keV.

The  $c$  coefficients for the 13 positive-parity levels discussed above are shown in Fig. 1. There is good agreement between experiment and theory except for the  $0^+$   $n = 10$  state. The energy of this state in  $^{30}\text{P}$  needs to be confirmed experimentally. As in Ref. [5] there is significant state dependence with  $c$  values from experiment ranging from about 170 keV to 276 keV. It is remarkable to observe that the cases with the smallest theoretical error based upon the differences between USDA-cdpn and USDB-cdpn ( $n = 1, 2, 4, 5$ ) are also those that have the best agreement with experiment.

A summary of the levels in  $^{30}\text{S}$  is given in Table II together with the calculated proton widths and  $\gamma$  widths. These serve as input to the reaction rate calculations. From the  $2^+$ ,  $n = 18$  level and beyond we use the energies and spins obtained with the USDB-cdpn Hamiltonian. Since the proton and gamma-decay widths are not measured in  $^{30}\text{S}$ , all of them are obtained from the USD(A)(B)-cdpn calculations. For the negative-parity states we take the experimental spectroscopic factors and gamma decay widths from their values in  $^{30}\text{Si}$ .

### III. COMPARISON WITH DATA FROM THE MIRROR NUCLEUS

We assess the agreement between our shell-model calculations and experiment, crucial to our method, by making comparisons to cases where experimental data is readily

TABLE II. Properties of states in  $^{30}\text{Si}$ .  $E_x(\text{th})$  are the USDB-cdpn theoretical excitation energies, and  $E_x(\text{exp})$  are taken from Table I. The state number  $n$  is in order of increasing experimental energy in  $^{30}\text{Si}$  as far as possible. The spectroscopic factors and gamma decay widths for positive-parity states are from the USDB-cdpn calculations. For negative-parity states experimental values for the mirror nucleus from Ref. [13] are used.

$n$	$J^\pi$	$k$	$E_x(\text{th})$ (MeV)	$E_x(\text{exp})$ (MeV)	$E_{\text{res}}$ (MeV)	$C^2S$		$\Gamma_\gamma$ (eV)	$\Gamma_p$ (eV)	$\omega\gamma$ (eV)
						$\ell = 0(1)$	$\ell = 2(3)$			
1	$0^+$	1	0.000	0.000		$8.4 \times 10^{-1}$				
2	$2^+$	1	2.244	2.210			$6.1 \times 10^{-1}$	$2.7 \times 10^{-3}$		
3	$2^+$	2	3.485	3.404			$9.2 \times 10^{-2}$	$4.8 \times 10^{-3}$		
4	$0^+$	2	3.871	3.668		$3.6 \times 10^{-1}$		$1.4 \times 10^{-4}$		
5	$1^+$	1	3.976	3.677		$6.0 \times 10^{-5}$	$6.0 \times 10^{-1}$	$2.7 \times 10^{-2}$		
6	$3^+$	1	4.825	4.688	0.288		$2.5 \times 10^{-2}$	$3.2 \times 10^{-3}$	$8.6 \times 10^{-6}$	$1.5 \times 10^{-5}$
7	$2^+$	3	4.805	4.809	0.409		$1.0 \times 10^{-1}$	$7.1 \times 10^{-3}$	$3.1 \times 10^{-3}$	$2.7 \times 10^{-3}$
8	$4^+$	1	5.278	5.132	0.732			$6.3 \times 10^{-3}$		
9	$0^+$	3	5.487	5.218	0.818	$3.0 \times 10^{-3}$		$5.2 \times 10^{-3}$	5.6	$1.3 \times 10^{-3}$
10	$3^+$	2	5.111	5.219	0.819		$2.0 \times 10^{-2}$	$2.3 \times 10^{-3}$	$5.7 \times 10^{-1}$	$4.0 \times 10^{-3}$
11	$3^-$	1		5.312	0.912		$4.0 \times 10^{-1}$	$1.1 \times 10^{-2}$	2.1	$1.9 \times 10^{-2}$
12	$2^+$	4	5.867	5.382	0.982		$5.6 \times 10^{-2}$	$5.2 \times 10^{-2}$	6.9	$6.5 \times 10^{-2}$
13	$4^+$	2	5.860	5.836	1.436			$2.6 \times 10^{-2}$		
14	$4^-$	1		6.225	1.825		$4.3 \times 10^{-1}$	$3.3 \times 10^{-3}$	$4.3 \times 10^2$	$7.4 \times 10^{-3}$
15	$1^-$	1		6.242	1.842	$3.3 \times 10^{-1}$		$3.3 \times 10^{-2}$	$2.6 \times 10^4$	$2.4 \times 10^{-2}$
16	$0^+$	4	6.725	6.326	1.926	$2.5 \times 10^{-3}$		$5.5 \times 10^{-2}$	$5.9 \times 10^2$	$1.4 \times 10^{-2}$
17	$2^-$	1		6.435	2.035	$8.6 \times 10^{-2}$		$2.2 \times 10^{-2}$	$1.1 \times 10^4$	$2.7 \times 10^{-2}$
18	$2^+$	5	6.497		2.097		$1.3 \times 10^{-2}$	$9.1 \times 10^{-2}$	$2.2 \times 10^2$	$1.1 \times 10^{-1}$
19	$3^+$	3	6.940		2.540		$3.8 \times 10^{-3}$	$3.1 \times 10^{-2}$	$1.6 \times 10^2$	$5.4 \times 10^{-2}$
20	$5^+$	1	6.996		2.596			$4.4 \times 10^{-3}$		

available, such as for the mirror nuclei. We compare theory to experimental data in the mirror nucleus  $^{30}\text{Si}$  in Tables III and IV, for spectroscopic factors for the reaction  $^{29}\text{Si}(d, p)^{30}\text{Si}$  and lifetimes of  $^{30}\text{Si}$ , respectively. The theoretical values are based on the USDA-cdpn and USDB-cdpn interactions.

Optimal  $g$  factors and effective charges for the  $\gamma$ -decay calculations are used that were determined from least-square fits to 48 magnetic moments, 26 quadrupole moments, 111  $M1$  transitions, and 144  $E2$  transitions [14] for USDA and USDB separately. The agreement between experimental and theory is

TABLE III. Spectroscopic factors for  $^{29}\text{Si}(d, p)^{30}\text{Si}$  from Ref. [13]. The convention for the state number  $n$  follows that of Table I.

$n$	$J^\pi$	$k$	$E_x$ uscb-cdpn (MeV)	$E_x$ exp (MeV)	$\ell$	$C^2S$		$C^2S$ exp
						USDA-cdpn	USDB-cdpn	
1	$0^+$	1	0.000	0.000	0	0.78	0.78	0.90
2	$2^+$	1	2.242	2.235	2	0.53	0.53	0.66
3	$2^+$	2	3.469	3.498	2	0.08	0.08	0.13
4	$1^+$	1	4.059	3.769	2	0.59	0.59	0.70
5	$0^+$	2	3.910	3.788	0	0.41	0.41	0.62
6	$2^+$	3	5.053	4.810	2	0.093	0.093	0.108
7	$3^+$	1	4.815	4.830	2	0.023	0.023	0.04
8	$3^+$	2	5.053	5.231	2	0.028	0.028	(0.007)
9	$4^+$	1	5.297	5.279				
10	$0^+$	3	5.408	5.372	0	0.008	0.008	weak
11	$3^-$	1		5.487	3			0.40
12	$2^+$	4	5.886	5.614	2	0.001	0.001	0.056
13	$4^+$	2	5.811	5.951				
14	$4^-$	1		6.503	3			0.43
15	$2^+$	5	6.434	6.537	2	0.0004	0.0004	0.008
16	$2^-$	1		6.641				0.086
17	$0^+$	4	6.740	6.642				
18	$1^-$	1		6.744	1			0.33

TABLE IV. Lifetimes for  $^{30}\text{S}$  and  $^{30}\text{Si}$  levels. The convention for the state number  $n$  follows that of Table I. Experimental results for  $^{30}\text{Si}$  are from Ref. [13].

$n$	$J^\pi$	$k$	$E_x[^{30}\text{Si}](\text{MeV})$		$T_{1/2}[^{30}\text{Si}](\text{fsec})$			$T_{1/2}[^{30}\text{S}](\text{fsec})$	
			USDB-cdpn	exp	USDA-cdpn	USDB-cdpn	exp	USDA-cdpn	USDB-cdpn
2	$2^+$	1	2.242	2.235	189	203	215(28)	154	171
3	$2^+$	2	3.469	3.498	41	45	58(17)	76	94
4	$1^+$	1	4.059	3.769	29	24	36(9)	12	11
5	$0^+$	2	3.910	3.788	8100	6200	8300(500)	5600	3300
6	$2^+$	3	5.053	4.810	86	81	104(15)	91	64
7	$3^+$	1	4.815	4.830	88	84	83(24)	118	144
8	$3^+$	2	5.053	5.231	115	118	43(21)	171	202
9	$4^+$	1	5.297	5.279	273	246	83(22)	118	73
10	$0^+$	3	5.408	5.372	85	97	59(21)	141	88
11	$3^-$	1		5.487			43(12)		
12	$2^+$	4	5.886	5.614	12	10	< 21	9	9
13	$4^+$	2	5.811	5.951	14	14	15(8)	15	18
14	$4^-$	1		6.503			139(35)		
15	$2^+$	5	6.434	6.537	4.0	4.8	< 17	3.8	5.0
16	$2^-$	1		6.641			21		
17	$0^+$	4	6.740	6.642	38	41		36	8.4
18	$1^-$	1		6.744			< 14		

excellent in most cases. The worst agreement for gamma decay is for the  $4^+$   $n = 9$  state. However, this state does not enter into the  $rp$  reaction rate because the  $sd$ -shell spectroscopic factor is zero [in agreement a very small experimental cross section in  $^{29}\text{Si}(d, p)$  that must come from a small  $\ell = 4$  admixture].

The lifetimes for the  $^{30}\text{S}$  levels are also given in Table IV. There is a mirror asymmetry in the calculated lifetime values due to the interference between the isoscalar and isovector components of the electromagnetic operator. For this reason, using information on the gamma decay of the neutron-rich nucleus ( $^{30}\text{Si}$ ) to obtain the  $(p, \gamma)$  rate in the proton-rich nucleus ( $^{30}\text{S}$ ) may be incorrect by up to a factor of two.

The fact that the interactions USDA-cdpn and USDB-cdpn generally give a good reproduction for the mirror nucleus of the crucial parameters in a rate calculation, namely single-nucleon spectroscopic factors and lifetimes, suggests that the results for  $^{30}\text{S}$  should be of similar quality. This supports the use of calculated values for these parameters for  $^{30}\text{S}$  when the experimental values are not available, as we have done by relying on calculated values for the spectroscopic factors and lifetimes given in Table I.

In the absence of calculations for the negative-parity states, we use the measured  $^{29}\text{Si} \rightarrow ^{30}\text{Si}$  spectroscopic factors (Table III), and the experimental gamma-decay lifetimes measured in  $^{30}\text{Si}$  (Table IV) for those in  $^{30}\text{S}$ ; however, the rate in the T9 region of interest in this case is dominated by the positive-parity states.

#### IV. RESULTS FOR THE REACTION RATE

The resonant reaction rate for capture on a nucleus in an initial state  $i$ ,  $N_A \langle \sigma v \rangle_{res i}$  for isolated narrow resonances is calculated as a sum over all relevant compound nucleus states

$f$  above the proton threshold [16]

$$N_A \langle \sigma v \rangle_{res i} = 1.540 \times 10^{11} (\mu T_9)^{-3/2} \times \sum_f \omega \gamma_{if} e^{-E_{res}/(kT)} \text{ cm}^3 \text{ s}^{-1} \text{ mole}^{-1}. \quad (4)$$

Here  $T_9$  is the temperature in GigaK,  $E_{res} = E_f - E_i$  is the resonance energy in the center of mass system, the resonance

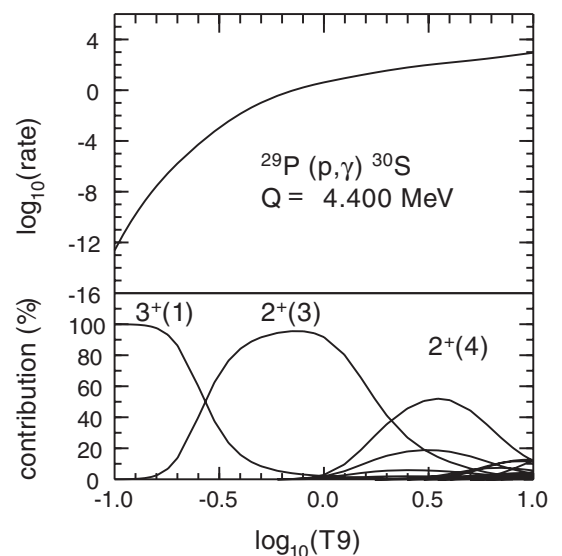


FIG. 2. The total  $rp$  reaction rate versus temperature  $T_9$  (GigaK) (top panel) and the contribution of each of the final states (lower panel) obtained with the data from Table II.



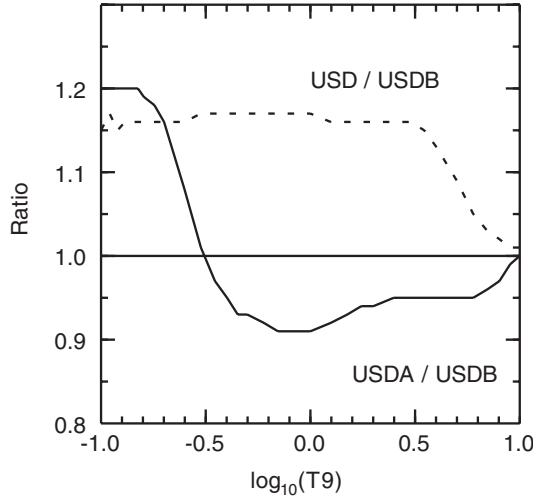


FIG. 3. The total  $rp$  reaction rates of USDA-cdpn, and USD-cdpn compared to USDB-cdpn for  $^{30}\text{S}$ .

strengths in MeV for proton capture are

$$\omega\gamma_{if} = \frac{(2J_f + 1)}{(2J_p + 1)(2J_i + 1)} \frac{\Gamma_{pif}\Gamma_{\gamma f}}{\Gamma_{\text{total } f}}. \quad (5)$$

$\Gamma_{\text{total } f} = \Gamma_{pif} + \Gamma_{\gamma f}$  is the total width of the resonance level and  $J_i$ ,  $J_p$ , and  $J_f$  refer to the target, the proton projectile ( $J_p = 1/2$ ), and states in the final nucleus, respectively. The proton decay width depends exponentially on the resonance energy via the single-particle proton width and can be calculated from the proton spectroscopic factor  $C^2S_{if}$  and the single-particle proton width  $\Gamma_{\text{sp}if}$  as  $\Gamma_{pif} = C^2S_{if}\Gamma_{\text{sp}if}$ . The method for calculating the single-particle proton widths is explained in Ref. [3].

The total  $rp$  reaction rates have been calculated for the interactions USDA-cdpn, USDB-cdpn, and USD-cdpn. Figure 2 shows the results for the resonance-capture rate

TABLE V. Properties of states in  $^{30}\text{S}$  that are most important for the  $p\gamma$  rate compared between the three Hamiltonians. The convention for the state number  $n$  follows that of Table II.

	$n$	$J^\pi$	$k$	$\Gamma_\gamma$ (eV)	$\Gamma_p$ (eV)	$\omega\gamma$ (eV)
USDA-cdpn	6	$3^+$	1	$3.9 \times 10^{-3}$	$10 \times 10^{-6}$	$1.8 \times 10^{-5}$
	7	$2^+$	3	$5.0 \times 10^{-3}$	$3.2 \times 10^{-3}$	$2.4 \times 10^{-3}$
	9	$0^+$	3	$3.2 \times 10^{-3}$	13	$0.8 \times 10^{-3}$
	10	$3^+$	2	$2.7 \times 10^{-3}$	$6.2 \times 10^{-1}$	$4.7 \times 10^{-3}$
	12	$2^+$	4	$5.0 \times 10^{-2}$	8.2	$6.2 \times 10^{-2}$
USDB-cdpn	6	$3^+$	1	$3.2 \times 10^{-3}$	$8.6 \times 10^{-6}$	$1.5 \times 10^{-5}$
	7	$2^+$	3	$7.1 \times 10^{-3}$	$3.1 \times 10^{-3}$	$2.7 \times 10^{-3}$
	9	$0^+$	3	$5.2 \times 10^{-3}$	5.6	$1.3 \times 10^{-3}$
	10	$3^+$	2	$2.3 \times 10^{-3}$	$5.7 \times 10^{-1}$	$4.0 \times 10^{-3}$
	12	$2^+$	4	$5.2 \times 10^{-2}$	6.9	$6.5 \times 10^{-2}$
USD-cdpn	6	$3^+$	1	$3.4 \times 10^{-3}$	$10 \times 10^{-6}$	$1.7 \times 10^{-5}$
	7	$2^+$	3	$8.8 \times 10^{-3}$	$3.5 \times 10^{-3}$	$3.2 \times 10^{-3}$
	9	$0^+$	3	$4.7 \times 10^{-3}$	0.05	$1.1 \times 10^{-3}$
	10	$3^+$	2	$2.3 \times 10^{-3}$	$4.3 \times 10^{-1}$	$4.0 \times 10^{-3}$
	12	$2^+$	4	$6.6 \times 10^{-2}$	7.9	$8.2 \times 10^{-2}$

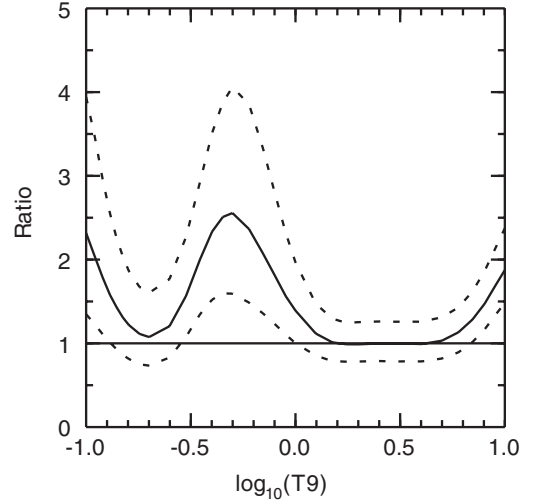


FIG. 4. The USDB-cdpn present rate divided by the rate given in the 2010 evaluation [15]; solid line for the median rate and the dashed lines for the low and high rates as given in Table B.58 of Ref. [15].

obtained using USDB-cdpn. The three dominant resonances are  $3^+(1)$ ,  $2^+(3)$ , and  $2^+(4)$ . The importance of the  $3^+(1)$  and  $2^+(3)$  states was noted in Ref. [17].

The uncertainty in the rate due to the use of different  $sd$ -shell Hamiltonians is about 20% as shown by the ratios in Fig. 3. The detailed differences for the most important states are given in Table V. The  $\ell = 0$  spectroscopic factor for the  $0^+$  state is very small (see Table III) and this gives a large spread in the calculated  $\Gamma_p$  values, but the  $\omega\gamma$  value is dominated by the smaller  $\Gamma_\gamma$  and it is relatively unimportant for the total rate. Experiments that are sensitive to differences of the values given in Table V could validate or perhaps reduce the uncertainty in the rate.

The main differences with the results of Almaraz-Calderon *et al.*, as given in Table VI of their paper [1], is that their  $\Gamma_p$  for the 5.130 MeV  $4^+$  is much too large since they incorrectly took  $\ell = 2$  (rather than  $\ell = 4$ ) [18]. Since this is a weak  $\ell = 4$  transition, its contribution to the  $rp$  rate is negligible, and it is not included in our rate. Also they do not include the 5.219 MeV  $3^+$  state from Lotay *et al.* [2]. The USDB-cdpn rate is compared to that of the 2010 evaluation (Table B.58 of Ref. [15]) in Fig. 4. For  $\log_{10}(T9) < 0$  our rate is up to a factor of 2.5 larger than the 2010 evaluation.

## V. CONCLUSIONS

The calculation of the  $rp$  reaction rate for the  $^{29}\text{P}(p,\gamma)^{30}\text{S}$  requires a knowledge of the energy levels in  $^{30}\text{S}$  above the proton-emission threshold of 4.400 MeV where the reaction rate is dominated by a few resonances. The energies used for  $^{30}\text{S}$  above the proton-emission threshold were all based on recent measurements which extend the known excitation energy spectrum to seven MeV. We first established the isobaric triplet assignments for  $A = 30$ . We have modified several assignments for the  $T = 1$  states in  $^{30}\text{P}$ , and have demonstrated that a good correspondence between theoretical and experimental values of the  $c$  coefficients for most states

up to 7 MeV in excitation energy for  $^{30}\text{S}$  can be obtained. The experimental spectroscopic factors for  $^{29}\text{Si} \rightarrow ^{30}\text{Si}$  and experimental  $\gamma$ -decay lifetimes for  $^{30}\text{Si}$  were in good agreement with the calculations. We obtained the  $^{29}\text{P}(p,\gamma)^{30}\text{S}$  rate based upon the calculated  $^{29}\text{P} \rightarrow ^{30}\text{S}$  spectroscopic factors and  $^{30}\text{S}$  lifetimes, together with the experimental energies. The  $rp$  rate has an error of about 20% due to the uncertainties in the  $sd$ -shell Hamiltonian. The present results for the  $^{29}\text{P}(p,\gamma)^{30}\text{S}$  rate should be the best currently available. For  $\log_{10}(T9) < 0$

our rates are up to a factor of 2.5 larger than those given by the 2010 evaluation [15].

#### ACKNOWLEDGMENTS

This work is partly supported by NSF Grant No. PHY-1068217, the Joint Institute for Nuclear Astrophysics NSF Grant No. PHY08-22648, and the National Research Foundation of South Africa Grant No. 76898.

- 
- [1] S. Almaraz-Calderon, W. P. Tan, A. Aprahamian, M. Beard, G. P. A. Berg, B. Bucher, M. Couder, J. Gorres, S. O'Brien, D. Patel, A. Roberts, K. Sault, M. Wiescher, C. R. Brune, T. N. Massey, K. Fujita, K. Hatanaka, D. Ishiwaka, H. Matsubara, H. Okamura, H. J. Ong, Y. Sakemi, Y. Shimizu, T. Suzuki, Y. Tameshige, A. Tamii, J. Zenihiro, T. Kubo, Y. Namiki, Y. Ohkuma, Y. Shimbara, S. Suzuki, R. Watanabe, R. Yamada, T. Adachi, Y. Fujita, H. Fujita, M. Dozono, and T. Wakasa, *Phys. Rev. C* **86**, 065805 (2012).
- [2] G. Lotay, J. P. Wallace, P. J. Woods, D. Seweryniak, M. P. Carpenter, C. J. Chiara, D. T. Doherty, R. V. F. Janssens, T. Lauritsen, A. M. Rogers, and S. Zhu, *Phys. Rev. C* **86**, 042801(R) (2012).
- [3] W. A. Richter, B. A. Brown, A. Signoracci, and M. Wiescher, *Phys. Rev. C* **83**, 065803 (2011).
- [4] B. A. Brown and W. A. Richter, *Phys. Rev. C* **74**, 034315 (2006).
- [5] W. E. Ormand and B. A. Brown, *Nucl. Phys. A* **491**, 1 (1989).
- [6] B. Ramstein, L. H. Rosier, and R. J. De Meijer, *Nucl. Phys. A* **363**, 110 (1981).
- [7] K. Setoodehnia, A. A. Chen, J. Chen, J. A. Clark, C. M. Deibel, S. D. Geraedts, D. Kahl, P. D. Parker, D. Seiler, and C. Wrede, *Phys. Rev. C* **82**, 022801(R) (2010).
- [8] W. A. Richter and B. A. Brown, *Phys. Rev. C* **85**, 045806 (2012).
- [9] C. Iliadis, P. M. Endt, N. Prantzos, and W. J. Thompson, *Astrophys. J.* **524**, 434 (1999).
- [10] M. Shamsuzzoha Basunia, *Nucl. Data Sheets* **111**, 2331 (2010).
- [11] C. A. Grossmann, M. A. LaBonte, G. E. Mitchell, J. D. Shriner, J. F. Shriner, G. A. Vavrina, and P. M. Wallace, *Phys. Rev. C* **62**, 024323 (2000).
- [12] B. A. Brown and B. H. Wildenthal, *Ann. Rev. of Nucl. Part. Sci.* **38**, 29 (1988).
- [13] P. M. Endt, J. Blachot, R. B. Firestone, and J. Zipkin, *Nucl. Phys. A* **633**, 1 (1998).
- [14] W. A. Richter, S. Mkhize, and B. A. Brown, *Phys. Rev. C* **78**, 064302 (2008).
- [15] C. Iliadis, R. Longland, A. E. Champagne, A. Coc, and R. Fitzgerald, *Nucl. Phys. A* **841**, 31 (2010).
- [16] W. A. Fowler and F. Hoyle, *Astrophys. J. Suppl.* **9**, 201 (1964).
- [17] C. Iliadis, J. M. D'Auria, S. Starrfield, W. J. Thompson, and M. Wiescher, *Astrophys. J. Suppl. Ser.* **134**, 151 (2001).
- [18] M. Wiescher (private communication).